Optimized prodigiosin production with *Pseudomonas putida* KT2440 using parallelized non-invasive online monitoring

Carl Brehl[a,b,#], Hannah U. C. Brass[b,c,#], Clara Lüchtrath[a], Lukas Böckmann[a], Nina Ihling[a,b], Thomas Classen[b,d], Jörg Pietruszka[b,c,d], Jochen Büchs[a,b*]

[a] AVT - Biochemical Engineering, RWTH Aachen University, Forckenbeckstraße 51, 52074 Aachen, Germany

[b] Bioeconomy Science Center (BioSC), Forschungszentrum Jülich GmbH, Jülich, Germany

[c] Institute of Bioorganic Chemistry, Heinrich Heine University Düsseldorf located at Forschungszentrum Jülich, Stetternicher Forst, 52426 Jülich, Germany

[d] Institute for Bio- and Geosciences 1: Bioorganic Chemistry (IBG-1), Forschungszentrum Jülich GmbH, 52428 Jülich, Germany

[#] The authors contributed equally.

Email addresses:

*Corresponding author: Jochen Büchs, RWTH Aachen University, AVT—Biochemical Engineering, Forckenbeckstraße 51, 52074 Aachen, Germany. Email: Jochen.Buechs@avt.rwth-aachen.de

Abstract

The red pigment prodigiosin is of high pharmaceutical interest, due to its potential applications as an antitumor drug and antibiotic agent. As previously demonstrated *Pseudomonas putida* KT2440 is a suitable host for prodigiosin production, as it exhibits high tolerance towards the antimicrobial properties of prodigiosin. So far, prodigiosin concentrations of up to 94 mg/L have been achieved in shake flask cultivations. For the characterization and optimization of the prodigiosin production process, the scattered light of *P. putida* and fluorescence of prodigiosin was measured. The excitation and emission wavelengths for prodigiosin measurement were analyzed by recording 2D fluorescence spectra. The strongest prodigiosin fluorescence was obtained at a wavelength combination of 535/560 nm. By reducing the temperature to 18 °C and using 16 g/L glucose, the prodigiosin concentration was more than doubled compared to the initial cultivation conditions. The obtained results demonstrate the capabilities of parallelized microscale cultivations combined with non-invasive online monitoring of fluorescence for rapid bioprocess development, using prodigiosin as a molecule of current biotechnological interest.

Keywords: BioLector, *Pseudomonas putida*, prodigiosin, online monitoring, microtiter plate,

1 Introduction

The bright red-colored natural product prodigiosin is a prominent member of the prodiginine class and is produced by various bacteria, including *Serratia marcescens* (*S. marcescens*) and *Hahella chejuensis* (*H. chejuensis*) [1-4]. Prodiginines exhibit various biological activities as antibiotic and antimalarial compounds, anti-cancer compounds, autophagy modulating compounds, and compounds against plant pathogenic nematodes and fungi [5-12]. Hence the prodiginine prodigiosin is of significant interest for novel drug development [13].

In earlier work, a sustainable and safe biotechnological production of prodigiosin was already established by Domröse et al. [14]. Due to its high tolerance against xenobiotics as a result of an efficient efflux system, *Pseudomonas putida* KT2440 (*P. putida*) was selected for heterologous prodigiosin production [15,16]. Consequently, the prodigiosin biosynthesis gene cluster (*pig* cluster) from the opportunistic human pathogen *S. marcescens* was chromosomally integrated into the safe production strain *P. putida* KT2440, resulting in the heterologous prodigiosin producer *P. putida* pig-r2 [14]. First experiments already evaluated the potential of the prodigiosin producer strain *P. putida* pig-r2 in terms of prodigiosin production. Optimization of cultivation parameters has resulted in titers of up to 94 mg/L prodigiosin in the fermentation broth. The optimization of prodigiosin production is of high scientific interest, which is reflected in the large number of studies on improved cultivation conditions[4]. However, systematic investigations of the cultivation conditions using online measurement techniques have the potential to enable the production of larger amounts of the bioactive natural product prodigiosin.

The first time reported in literature, prodigiosin fluorescence was measured at an excitation wavelength (ex) of 543 nm and an emission wavelength (em) of 570 nm [17]. Additionally Andreyeva and Ogorodnikova [18] reported a fluorescence measurement for prodigiosin produced by *S. marcescens* at an wavelength combination of 535 nm (ex) and 560–565nm (em). In a more recent study, prodigiosin was measured by a HPLC using a fluorescent detector with

(ex/em) 535/555 nm[19]. Therefore, its fluorescence makes prodigiosin an excellent candidate for combination of fluorescence monitoring and high-throughput cultivation in microtiter plates (MTPs) for optimization of product formation. Small scale online monitoring and optimization tasks have been addressed in multiple studies using MTP-based online monitoring systems [20-23]. However complex media as used by Domröse et al. contain complex compounds (e.g., NADH, riboflavin) that are known to interfere with the fluorescence measurements[14]. In contrast, mineral media have this disadvantage to a lesser extent. Additionally, mineral media have a defined composition, and offer advantages when isolating the natural product from the culture [24-26]. Furthermore, mineral media would enable potential future flux analysis and labelling experiments [27]. Consequently, cultivation in a mineral medium is expected to be advantageous for prodigiosin production.

It is the aim of this study to establish an online monitoring setup for prodigiosin in MTPs using a mineral medium. For this purpose, an in-house built device for fluorescence measurement in MTPs is utilized. It allows the free selection of the measured wavelength combinations [21]. The established measurement window will be used to optimize the cultivation conditions of *P. putida* pig-r2 for the prodigiosin production concerning the temperature and glucose concentration.

2 Material & Methods

2.1 Microorganisms

P. putida KT2440 (wild type) and *P. putida* pig-r2 (prodigiosin production strain) were received from the Institute of Molecular Enzyme Technology, Heinrich Heine University Düsseldorf located at Forschungszentrum Jülich, Jülich, Germany. *P. putida* pig-r2 is described in detail by Domröse et al. [14,28].

2.2 Media composition

All components were either purchased from Carl Roth GmbH & Co. KG (Karlsruhe, Germany), Sigma Aldrich Chemie GmbH (Darmstadt, Germany), or Merck KGaA (Darmstadt, Germany), if not stated otherwise. The Delft medium was adapted from Hartmans, Smits, Van der Werf, Volkering and De Bont [29]. It was prepared as follows: 10 mL/L of 100× buffer solution (388 g/L K_2HPO_4, 163 g/L NaH_2PO_4), 10 mL/L of 100× $(NH_4)_2SO_4$ solution [200 g/L $(NH_4)_2SO_4$], and 10 mL/L of 100× minimal salt solution (1 g/L $Na_2EDTA \cdot 2\ H_2O$, 10 g/L $MgCl_2 \cdot 6\ H_2O$, 500 mg/L $FeSO_4 \cdot 7\ H_2O$, 200 mg/L $ZnSO_4 \cdot 7\ H_2O$, 100 mg/L $CaCl_2 \cdot 2\ H_2O$, 100 mg/L $MnCl_2 \cdot 2\ H_2O$, 20 mg/L $Na_2MoO_4 \cdot 2\ H_2O$, 20 mg/L $CuSO_4 \cdot 2\ H_2O$, 47 mg/L $CoSO_4 \cdot 7\ H_2O$) were diluted with deionized H_2O. For the preparation of the 100× minimal salt solution, EDTA was first completely dissolved before all other components were added. Therefore, 25 mL deionized H_2O were added to 1 g EDTA. Afterwards, 10 M NaOH was added until the EDTA was completely dissolved. This solution was added to the remaining required water and the remaining salts for preparation of the 100× minimal salt solution. The pH value was adjusted to pH 4 using concentrated HCl.

The M9 medium was adapted from Sambrook et al. [30]. It was prepared as follows: 8.5 g/L $Na_2HPO_4 \cdot 2\ H_2O$, 3 g/L KH_2PO_4, 0.5 g/L NaCl, and 1 g/L NH_4Cl were dissolved in distilled H_2O and supplemented with 2 mL/L $MgSO_4$ solution (120.16 g/L) and 1 mL/L US trace

element solution (82.81 mL/L 37% HCl, 4.87 mg/L $FeSO_4 \cdot 7\ H_2O$, 4.12 g/L $CaCl_2 \cdot 2\ H_2O$, 1.87 g/L $ZnSO_4 \cdot 7\ H_2O$, 1.5 g/L $MnCl_2 \cdot 4\ H_2O$, 0.84 g/L $Na_2EDTA \cdot 2\ H_2O$, 0.3 g/L H_3BO_3, 0.25 g/L $Na_2MoO_4 \cdot 2\ H_2O$ and 0.15 g/L $CuCl_2 \cdot 2\ H_2O$). The pH value was adjusted to 7 with 1 M KOH.

The Wilms-MOPS medium was adapted from Schiedle et al. [31]. It was prepared as follows: 400 mL/L of MOPS stock solution (105 g/L), 20 mL/L of phosphate stock solution (150 g/L K_2HPO_4), 20 mL/L of 50× nitrogen-stock [250 g/L $(NH_4)_2SO_4$, 25 g/L NH_4Cl], 20 mL/L of 50× Na-stock (100 g/L Na_2SO_4), 10 mL/L of 50× Mg-stock (50.0 mg/L $MgSO_4 \cdot 7\ H_2O$) and 1 mL/L of 1000× trace element solution (41.8 g/L $FeCl_3 \cdot 6\ H_2O$, 33.4 g/L EDTA, 1.98 g/L $CaCl_2 \cdot 2\ H_2O$, 640 mg/L $CoSO_4 \cdot 7\ H_2O$, 540 mg/L $ZnSO_4 \cdot 7\ H_2O$, 310 mg/L $CuSO_4$, 300 mg/L $MnSO_4 \cdot H_2O$) were mixed and filled up to 1 L with deionized water.

The LB (lysogeny broth) liquid medium used for the first precultures in the media screening was prepared from 10 g/L tryptone, 5 g/L yeast extract, 10 g/L NaCl.

The modified M63 mineral medium derived from Elbing and Brent [32] consists of 200 mL/L M63 salt solution (10 g/L $(NH_4)_2SO_4$, 68 g/L KH_2PO_4), 1 mL/L $MgSO_4$ solution (120.16 g/L), and 1 mL/L US trace element solution. All chemicals were dissolved in deionized water. The pH value was adjusted to 7 with 1 M KOH.

For cultivations with *P. putida* pig-r2 two antibiotics, namely 1 mL/L gentamycin sulfate (stock with 10 g/L dissolved in deionized water) and 10 mL/L irgasan (stock with 10 g/L dissolved in 99% (*v/v*) ethanol), were added to the medium. For all cultivations 16 g/L glucose were added from a 500 g/L stock solution.

2.3 Online-measurement setup

All online monitored experiments were performed with an in-house built device for monitoring fluorescence and scattered light with a Fluoromax-4 spectrometer (HORIBA Jobin-Yvon GmbH, Bernsheim, Germany) in MTPs as described in detail by Wandrey et al. [21]. The data was obtained using the LabVIEW software developed by ZUMOLab GbR (Wessling, Germany). The device enables cultivations in 48-well MTPs with quasi-continuous and non-invasive measurement of scattered light and fluorescence. All main culture cultivations were performed in 48-well Flowerplates [33] (m2p-labs GmbH, Baesweiler, Germany). Each well of the MTP was filled with 800 µL of inoculated culture and shaken at 1000 rpm with a shaking diameter of 3 mm at a temperature of 15–30 °C. The scattered light was measured at an excitation wavelength (ex) of 650 nm and an emission wavelength (em) of 650 nm. The prodigiosin fluorescence was measured at ex/em 535/560 nm.

2.4 Data normalization

All online data were normalized to reference cultivations performed with *P. putida* pig-r2. The normalized online data were calculated according to formula (1). I_{max} was obtained at the end of the growth phase, at the point when scattered light and fluorescence reached their maximum (after ≈ 12 h; Suppl. Fig. 1 A). An example for the normalization can be found in Suppl. Fig. 1.

$$I_{norm} = \frac{I - I_0}{I_{max} - I_0} \quad (1)$$

I_{norm} = normalized intensity [-]

I = measured intensity [a.u.]

I_0 = intensity of the reference cultivation at the beginning ($t = 0$ h) [a.u.]

I_{max} = maximum intensity of reference cultivation (after ≈ 12 h; Suppl. Fig. 1 A) [a.u.]

2.5 Precultures

The precultures were performed in an in-house built RAMOS® device (Respiratory Activity Online Monitoring System) [34,35] and inoculated with 5 µL/mL from a cryo culture that had been stored at -80 °C. All precultures were carried out in 250 mL RAMOS®-flasks with a filling volume of 10 mL in modified M63 mineral medium at a shaking frequency of 300 rpm and a temperature of 30 °C. The precultures were cultivated for 12-18 h and stopped at the late exponential growth phase indicated by an oxygen transfer rate of 25-30 mmol/L/h (grey area in Suppl. Fig. 2). These synchronized precultures were used to inoculate the main culture with an initial optical density (OD_{650nm}) of 0.5. This procedure secured comparable cell growth over all the different experiments presented in Fig. 1 5.

2.6 2D fluorescent scan

The 2D fluorescent spectrum of pure prodigiosin (1 mg/L dissolved in DMSO) was measured in a Fluoromax-4 spectrometer (HORIBA Jobin-Yvon GmbH, Germany) in a quartz-glass cuvette. The prodigiosin was produced and purified via column chromatography as described in Domröse et al. and Brass et al. and the purity determined via qNMR measurements [14,36]. The spectrum was recorded at excitation wavelengths from 500 to 600 nm with a step size of 4 nm. The fluorescence emission was recorded at wavelengths from 500 to 600 nm with a step size of 4 nm for each excitation wavelength.

2D fluorescent spectra during main cultivation in modified M63 mineral medium in 48-well Flowerplates (m2p-labs GmbH, Baesweiler, Germany) were recorded every 45 min. The spectra were recorded at excitation wavelengths from 510 to 550 nm with a step size of 5 nm and emission wavelengths between 560 and 580 nm with a step size of 5 nm. The published fluorescence of prodigiosin at ex/em 543/570 nm [17] was also recorded as a reference.

2.7 Offline measurement

The OD_{650nm} was measured at a wavelength of 650 nm using a Genesys20 photometer (ThermoFischer, Schwerte, Germany). The prodigiosin concentration of each sample was analyzed using acidified ethanol extraction. For this purpose, the culture broth was centrifuged for 5 minutes at 14,000 rpm (Sigma1-15, Sigma, Darmstadt, Germany). The cell pellet was resuspended in acidified ethanol [4% (*v*/*v*) HCl (1 M) in ethanol], and the prodigiosin was dissolved and subsequently centrifuged for 5 min at 14,000 rpm. The supernatant was used to measure the prodigiosin absorbance at 535 nm using the Genesys20 photometer (ThermoFischer, Schwerte, Germany). The prodigiosin concentration was calculated with equation 2 using the molar extinction coefficient of prodigiosin previously determined with prodigiosin whose purity was assessed by qNMR[14].

$$\text{Prodigiosin concentration} = \frac{A_{535}}{\varepsilon} \cdot MW \quad (2)$$

A_{535}	Absorbance at 535 nm	[-]
ε	Extinction coefficient in acidified ethanol	[139,800 1/(M*cm)]
MW	Molecular mass prodigiosin	[323.43 g/mol]

2.8 HPLC analysis

The cell suspension was centrifuged at 14,000 rpm for 5 min. The supernatant was sterile-filtered into high-performance liquid chromatography (HPLC) vials and stored at 4 °C until analysis. The glucose analysis was performed in a HPLC system (Prominence HPLC, Shimadzu Deutschland, Duisburg, Germany) equipped with an ion-exclusion column (ROA-Organic Acid H+; Phenomenex Inc., Aschaffenburg, Germany) with 5 mM H_2SO_4 as a solvent and a flow

rate of 0.8 mL/min at 75 °C. A refractometer (RID-20A; Shimadzu Deutschland, Germany) was used for detection.

2.9 Initial media screening

Planning and evaluation of the data was carried out by using the program Design Expert 12 (Stat-Ease, Inc.) and central composite design. As numerical parameters, temperature (-α = 20 °C, +α = 37 °C) and glucose concentration (-α = 2.5 g/L, +α = 20 g/L) were analyzed. The four different mineral media (Delft mineral medium, M9 mineral medium, modified M63 mineral medium, and WilmsMOPS mineral medium) were analyzed as categorical parameter. The factorial points and axial points were performed in duplicates, whereas the central point was performed five times. Duplicates of the experiments at 18 °C and with a glucose concentration of 2.5 g/L, 5 g/L, 10 g/L, 15 g/L, and 20 g/L were added to the initial design and included in the evaluation. After performing the experiments suggested by the Design Expert 12 program (Stat-Ease, Inc., America, Minneapolis), the resulting values of the obtained prodigiosin concentration were entered into the program, and response-surface-graphs were obtained as output.

The cultivation experiments were performed as follows. Cultivation of the strain *P. putida* pig-r2 was performed in a BioLector® device [37] (m2p-labs GmbH, Baesweiler, Germany) . *P. putida* pig-r2 precultures were performed in LB liquid medium incubated at 30 °C overnight. Glucose (2.5–20 g/L) was added as a carbon source to the four examined mineral media. The media were inoculated with the *P. putida* pig-r2 preculture to an OD_{650} of 0.05. Cultivation of the main culture was performed according to 2.3.The cultivation temperature was varied between 18 and 37°C. As soon as the online measured scattered light indicated the stationary growth phase by reaching a constant plateau, the cultivation was stopped. For determining the amount of prodigiosin, 500 µL samples were taken and extracted

with acidic ethanol as described above. Sample treatment and calculation of the prodigiosin concentration was performed as described in section 2.7.

3 Results & discussion

3.1 Initial media screening

Initial optimization of the cultivation conditions in complex media of *P. putida* pig-r2 enabled prodigiosin titers of up to 94 mg/L [14]. Building on these experiments, the cultivation parameters were further analyzed in this study. For an initial media screening, four different mineral media were chosen instead of complex media. The results of the initial media screening (Suppl. Fig. 3) clearly showed that the highest prodigiosin titers were obtained using the modified M63 mineral medium at low cultivation temperatures of 18 °C and a glucose concentration around 15 g/L. These results formed the basis for further systematic investigations using the novel online fluorescence measurement method developed for prodigiosin.

3.2 Determination of optimum wavelength combinations for prodigiosin measurement

As a first step in developing an online measurement protocol, it is necessary to identify the fluorescent measurement range. Therefore, literature was reviewed to identify a suitable measurement range for determining the prodigiosin fluorescence. Tenconi et al. [17]and Andreyeva and Ogorodnikova [18] described a fluorescence of prodigiosin at an excitation wavelength of 543/535 nm and an emission wavelength between 560-570 nm. 2D fluorescent spectra were recorded to validate these wavelengths.

A first 2D fluorescent spectrum was obtained from pure prodigiosin dissolved in DMSO (1 mg/L) (Fig. 1A) This 2D fluorescent spectrum has a maximum fluorescence at excitation wavelengths from 536 nm to 545 nm and emits the most intense fluorescence between 563 nm and 572 nm. These results confirm the findings published by Tenconi et al. [17]. However, optimum wavelength combinations might differ between pure prodigiosin dissolved in DMSO

and prodigiosin in culture medium. Consequently, 2D fluorescent spectra were recorded during the cultivation of *P. putida* pig-r2 producing prodigiosin in modified M63 mineral medium. The 2D fluorescent spectra of prodigiosin during the cultivation (Fig. 1B) displayed a peak fluorescence intensity at an excitation wavelength of 535 nm and an emission wavelength of 560 nm. The red circle marks this peak, which differs from the published wavelength combination by Tenconi et al. [17] marked with a star symbol. The peak wavelength combination aligns with the findings of Andreyeva and Ogorodnikova [18]. However, the wavelength combination determined from the 2D-spectra in culture medium allows to obtain a 50% stronger signal during cultivation than the wavelength combination published by Tenconi et al. [17]. For validation, the two wavelengths were compared for a cultivation lasting 21 h (Suppl. Fig. 4). In addition to *P. putida* pig-r2, the two fluorescent wavelength combinations were measured for the prodigiosin non-producing wild-type strain of *P. putida* KT2440 to determine the background intensity. It is shown that the prodigiosin fluorescence can be clearly distinguished from the cellular background fluorescence of the wild-type strain for both wavelength combinations. The stronger wavelength combination (ex/em 535/565) showed a 50% overall stronger signal over the whole cultivation as well as a 20% increase of the signal-to-noise ratio compared to the wavelength combination of Tenconi et al. [17]. With the optimized wavelength combination for prodigiosin detection, the online measurement protocol was developed further.

3.3 Validation of an online screening protocol for prodigiosin

After determination of the ideal wavelength combination for online monitoring of prodigiosin production, an online screening protocol was established and validated using parallel offline measurements (Fig. 2). The OD_{650} (Fig. 2 A, blue stars) shows an instant exponential increase until 5 h after inoculation. Subsequently, the slope decreases, and the growth curve increases linearly. This indicates a limitation during the cultivation. The growth stops after 11 h, when the OD_{650} reaches a value of 12. The prodigiosin concentration (Fig 2 A, red squares) follows

the same trend as the growth of the culture. Prodigiosin production is thus obviously coupled to growth and is not formed after growth has stopped. The correlation between prodigiosin production and growth of *P. putida* pig-r2 may be due to the characteristics of the strain itself. Using the transfer and expression of biosynthetic pathways (TREX) system, the prodigiosin (pig) cluster necessary for prodigiosin production was inserted into *P. putida* KT2440, integrating into the 16S rRNA coding region of *rrnC*, one of the seven rRNA operons present in *P. putida* KT2440 [14,28,38-40]. It is assumed that the expression of bacterial *rrn* operons correlates with growth to provide a sufficient amount of ribosomes to meet the cells higher demand for proteins [28,41]. In this context, external factors such as nutrient deficiency or stress may also influence the expression [28,41-43]. Under the applied cultivation conditions, a maximum prodigiosin concentration of around 110 mg/L was obtained. The deviation of the prodigiosin concentration (98–118 mg/L) at the end of the cultivation (11–14 h) is most likely caused by deviations in the measurement procedure. The approximate final prodigiosin concentration could be confirmed in multiple experiments (data not shown). The glucose concentration (Fig. 2 A, green triangles) decreases exponentially for the first five to six hours. Until 11 hours, the glucose decrease follows a linear course, matching the course of the optical density over the cultivation time, as glucose is the main carbon source used for growth.

The scattered light and the prodigiosin fluorescence were measured every 1.5 min during the cultivation (Fig. 2 B) to gain more in-depth insights into the cultivation. The scattered light (Fig. 2 B, blue dotted line) increases exponentially for the first 5 h. Subsequently, the scattered light curve follows a linear course until it reaches its maximum after 11 h. Afterwards, the scattered light slightly decreases until the cultivation is stopped. The slight decrease is most likely a result of morphological changes of the *P. putida* cells after the carbon source is depleted at the end of the cultivation. This decrease has been shown by Geinitz et al. [20] for different organisms. The course of the scattered light matches well with the course of the offline

measured OD_{650}. Hence, it can be concluded that the measurement of scattered light at 650 nm is a well-suited online parameter to follow cell growth of the prodigiosin producing *P. putida* pig-r2 strain without sampling.

The second online measured parameter was the prodigiosin fluorescence (Fig. 2 B, red line). In addition, microscopic pictures of the cultures were taken at different time points (Fig. 2 C). For the first 2 h, an exponential increase of the online measured prodigiosin concentration can be seen. Afterwards, the curve reaches a plateau. During this time, the formation of small agglomerates and independent cells can be seen in the microscopic picture of the sample after 3 h (Fig. 2 C 1). The agglomerates have been observed for other prodiginines producers [10] and *Pseudomonas* strains [44]. The plateau is held for roughly 1 h, after which a short spike in the curve with an additional drop occurs (Fig. 2 B). After an additional 1 h, a steep signal drop occurs, and the signal loses about 40 % of its intensity. Here, the second microscopic picture was taken (Fig. 2 C 2). It can be seen that large agglomerates with a bright red color were formed. These agglomerates give a first explanation for the unsteady course of the online prodigiosin signal. It has been shown that large agglomerations can lead to a so-called inner filter effect. This phenomenon describes a reduction in the overall fluorescence signal caused by absorption of the fluorescent light [45]. The signal stays at a relative value of 0.4 for 30 min after which it increases again to the level before the drop. This plateau is held until a cultivation time of 10.5 h is reached. The signal then increases until it reaches a relative value of 0.9 at 11 h. Subsequently, the signal decreases slightly until it spikes to its maximum relative value of around 1 after 12 h. At this time point, the last microscopic sample was taken (Fig. 2 C 3). The agglomerates in this picture are smaller in size and more single cells can be seen. This supports the explanation that inner filter effects as a result of agglomeration are influencing the fluorescence signal of prodigiosin. After this final maximum, the online prodigiosin signal decreases again until the end of the cultivation. This course of the measured prodigiosin

fluorescence did not match the offline determined prodigiosin concentration (Fig. 2 A and B). However, the maximum online measured prodigiosin fluorescence correlates with the end of the cultivation and, thus, indicates the final and maximum prodigiosin concentration obtained during cultivation. In Suppl. Fig. 6, the online measured prodigiosin fluorescence is plotted for different glucose concentrations. This Figure shows a reproducible course of the prodigiosin fluorescence for the different glucose concentrations. The data indicates an increasing prodigiosin fluorescence up to a glucose concentration of 16 g/L. Hence, the more glucose was available, the more prodigiosin is produced. This trend is also seen in the offline samples in Fig 4. It can be concluded that the online prodigiosin fluorescence measurement allows for a semi-quantitative screening for improved process parameters.

3.4 Process optimization of prodigiosin production using the developed online screening protocol

The newly developed online prodigiosin measurement protocol was applied to optimize the cultivation conditions for the production of prodigiosin concerning the glucose concentration and the temperature. The modified M63 medium was used, as it has presented itself as the most promising medium (Suppl. Fig. 3). The results of the initial media screening (3.1) and previously published literature indicated a decreased prodigiosin titer at higher temperatures[14,46]. Therefore, the glucose concentration was varied from 6 to 18 g/L and the temperature from 18 to 30 °C (Fig. 3). It was found that the highest cultivation temperatures result in the lowest prodigiosin fluorescence (Fig. 3, blue areas). In contrast, the lowest temperatures result in the highest prodigiosin fluorescence (Fig. 3, red areas). Glucose concentrations of more than 14 g/L result in an increased prodigiosin fluorescence for all temperatures. Thus, the highest prodigiosin fluorescence was measured at a glucose concentration of 16 g/L at a temperature of 18 °C. These findings were also validated by the offline samples (Fig. 4). A maximum prodigiosin concentration of 210 mg/L was found under the applied conditions (15 g/L glucose; 18 °C). This result fits well with the temperature optimum of the enzyme that catalyzes the final reaction in prodigiosin biosynthesis, the condensation enzyme pigC [7,36,46-49]. It has been shown by You et al. [46] that the pigC enzyme has its temperature optimum between 10–20 °C. Other prodigiosin-producing strains such as *S. marcescens* have been reported to show still higher prodigiosin titers (more than 6 g/L), yet at the drawback of using an opportunistic pathogenic strain [4]. In addition to optimization of cultivation conditions, further genetic modification of *P. putida* strains has been shown to increase prodigiosin titers[50].

Subsequently, the space-time yield (STY) was calculated for this production process to evaluate the productivity of the process. Fig. 5 shows the STY for each point in Fig. 3. In contrast to the

product concentration, the STY presents a wider optimum. The highest STY is reached at 25 °C and 8 g/L glucose. However, at 18 °C and 6 g/L glucose, the second-highest STYs are reached. The lowest STYs are calculated for low temperatures and high glucose concentrations (e.g., 18 g/L glucose and 20 °C). For further process development and cultivation at larger scale, the setup time of the fermenter also has to be considered. This can increase the feasibility of a more protracted process with increased final product concentrations. The results presented in Fig. 5 indicate that further lowering of the cultivation temperature below 18 °C could lead to even higher product titers. However, the STY will decrease as growth is expected to slow down further. As a result of the decreasing economic efficiency, investigations and cultivations at temperatures below 18 °C have not been carried out.

The developed method for high-throughput online measurement of prodigiosin production in MTPs enabled identification of improved production conditions for prodigiosin in MTPs. At 18 °C with 16 g/L glucose as carbon source, it was possible to increase the prodigiosin concentrations 2-fold compared to previously published results by Domröse et al. [14].

4 Conclusion

In the present work, a semi-quantitative online measurement setup for determination of prodigiosin was developed. The prodigiosin detection was validated during cultivations of *P. putida* pig-r2 in a mineral medium using online fluorescence measurements. Initially, different media were screened using a design of experiments approach. The modified M63 mineral medium was selected for further development of an online measurement setup. For monitoring, an in-house-built device for monitoring fluorescence and scattered light in MTPs was applied. A 1.5 times stronger fluorescence of prodigiosin fluorescence was measured at a wavelength combination of 535/560 nm during cultivations compared to published prodigiosin fluorescence wavelength combinations. The optimized wavelength combination was exploited to establish a non-invasive online measurement for prodigiosin. Offline samples were used to validate the online quantification. By reduction of the temperature to 18 °C and the use of the modified M63 mineral medium, the prodigiosin titer was more than doubled compared to the initial cultivation conditions at 20 °C in complex medium [14].

With the newly established methodology for online monitoring of the prodigiosin concentration in MTPs, rapid process development and media optimization can be carried out in future experiments. In a next step, the applicability of the online measurement of prodigiosin has to be demonstrated also for other strains.

Abbreviations

pig cluster	Prodigiosin biosynthesis gene cluster
ex	Excitation wavelength
em	Emission wavelength
RAMOS	Respiratory activity online monitoring system
OTR	Oxygen transfer rate
OD_{650nm}	Optical density
MTP	Microtiter plate
HPLC	High performance liquid chromatography
STY	Space-time yield
TREX system	transfer and expression of biosynthetic pathways system

Acknowledgments

This research was funded by the Ministry of Culture and Science within the framework ofthe NRW-Strategieprojekt Bioeconomy Science Center (BioSC, no. 313/323-400-002 13).

Conflict of interests

The authors declare that they have no conflict of interests

Author contributions

CB and HB contributed equally to this study. CB and HB designed the study. HB and TC planned the initial media screening. HB performed the initial media screening. CB and CL performed experiments for the development of the online monitoring. CB and HB analyzed the data and drafted the manuscript. NI, JP and JB initiated and supervised the study, participated

in data interpretation and assisted in drafting the manuscript. All authors read and approved the final manuscript

References

1. Fürstner A. Chemie und Biologie des Roseophilins und der Prodigiosin-Alkaloide: 2500 Jahre im Überblick. *Angewandte Chemie*. 2003;115(31):3706-3728. doi:10.1002/ange.200300582
2. Hu DX, Withall DM, Challis GL, Thomson RJ. Structure, Chemical Synthesis, and Biosynthesis of Prodiginine Natural Products. *Chem Rev*. 2016;116(14):7818-53. doi:10.1021/acs.chemrev.6b00024
3. Williamson NR, Fineran PC, Leeper FJ, Salmond GP. The biosynthesis and regulation of bacterial prodiginines. *Na Rev Microbiol.* 2006;4(12):887-99. doi:10.1038/nrmicro1531
4. Han R, Xiang R, Li J, Wang F, Wang C. High-level production of microbial prodigiosin: A review. *J Basic Microbiol*. Jun 2021;61(6):506-523. doi:10.1002/jobm.202100101
5. Habash SS, Brass HU, Klein AS, et al. Novel prodiginine derivatives demonstrate bioactivities on plants, nematodes, and fungi. *Front Plant Sci*. 2020;11
6. Klein AS, Domröse A, Bongen P, et al. New prodigiosin derivatives obtained by mutasynthesis in *Pseudomonas putida*. *ACS Synth Biol*. 2017;6(9):1757-1765.
7. Klein AS, Brass HUC, Klebl DP, et al. Preparation of Cyclic Prodiginines by Mutasynthesis in *Pseudomonas putida* KT2440. *ChemBioChem*. 2018;19(14):1545-1552. doi:10.1002/cbic.201800154
8. Zhao C, Qiu SZ, He J, et al. Prodigiosin impairs autophagosome-lysosome fusion that sensitizes colorectal cancer cells to 5-fluorouracil-induced cell death. *Cancer Lett.* 2020;481:15-23. doi:10.1016/j.canlet.2020.03.010
9. Papireddy K, Smilkstein M, Kelly JX, et al. Antimalarial activity of natural and synthetic prodiginines. *J Med Chem*. 2011;54(15):5296-5306.
10. Stankovic N, Senerovic L, Ilic-Tomic T, Vasiljevic B, Nikodinovic-Runic J. Properties and applications of undecylprodigiosin and other bacterial prodigiosins. *App Microbiol Biotechnol.* 2014;98(9):3841-3858. doi:10.1007/s00253-014-5590-1
11. Pérez-Tomás R, Montaner B, Llagostera E, Soto-Cerrato V. The prodigiosins, proapoptotic drugs with anticancer properties. *Biochem Pharmacol*. 2003;66(8):1447-1452.
12. Berning L, Schlütermann D, Friedrich A, et al. Prodigiosin Sensitizes Sensitive and Resistant Urothelial Carcinoma Cells to Cisplatin Treatment. *Molecules*. 2021;26(5):1294. doi:10.3390/molecules26051294
13. Paul T, Bandyopadhyay TK, Mondal A, Tiwari ON, Muthuraj M, Bhunia B. A comprehensive review on recent trends in production, purification, and applications of prodigiosin. *Biomass Conv Bioref*. 2020;doi:10.1007/s13399-020-00928-2
14. Domröse A, Klein AS, Hage-Hülsmann J, et al. Efficient recombinant production of prodigiosin in *Pseudomonas putida*. *Front Microbiol*. 2015/09/15/ 2015;6doi:10.3389/fmicb.2015.00972
15. Dos Santos VA, Heim S, Moore ER, Stratz M, Timmis KN. Insights into the genomic basis of niche specificity of *Pseudomonas putida* KT2440. *Environ Microbiol*. 2004;6(12):1264-86. doi:10.1111/j.1462-2920.2004.00734.x
16. Fernández M, Duque E, Pizarro-Tobías P, Van Dillewijn P, Wittich RM, Ramos JL. Microbial responses to xenobiotic compounds. Identification of genes that allow *Pseudomonas putida* KT2440 to cope with 2, 4, 6-trinitrotoluene. *Microb Biotechnol*. 2009;2(2):287-294.
17. Tenconi E, Guichard P, Motte P, Matagne A, Rigali S. Use of red autofluorescence for monitoring prodiginine biosynthesis. *J Microbiol Meth*. 2013/05// 2013;93(2):138-143. doi:10.1016/j.mimet.2013.02.012
18. Andreyeva IN, Ogorodnikova TI. Pigmentation of *Serratia marcescens* and spectral properties of prodigiosin. *Microbiology*. 2015/01// 2015;84(1):28-33. doi:10.1134/S0026261715010026
19. Aboras S, Korany M, Abdine H, Ragab M, El Diwany A, Agwa M. HPLC with fluorescence detection for the bioanalysis and pharmacokinetic study of Doxorubicin and Prodigiosin loaded on eco-friendly casein nanomicelles in rat plasma. *J Chromatogr B Analyt Technol Biomed Life Sci*.;1187:123043. doi:10.1016/j.jchromb.2021.123043
20. Geinitz B, Rehmann L, Büchs J, Regestein L. Noninvasive tool for optical online monitoring of individual biomass concentrations in a defined coculture. *Biotech Bioeng*. 2020;117(4):999-1011. doi:10.1002/bit.27256
21. Wandrey G, Bier C, Binder D, et al. Light-induced gene expression with photocaged IPTG for induction profiling in a high-throughput screening system. *Microb Cell Fact*. 2016;15(1)doi:10.1186/s12934-016-0461-3
22. Ladner T, Held M, Flitsch D, Beckers M, Büchs J. Quasi-continuous parallel online scattered light, fluorescence and dissolved oxygen tension measurement combined with monitoring of the oxygen transfer rate in each well of a shaken microtiter plate. *Microb Cell Fact*. 2016;15(1):206. doi:10.1186/s12934-016-0608-2
23. Mühlmann M, Forsten E, Noack S, Büchs J. Optimizing recombinant protein expression via automated induction profiling in microtiter plates at different temperatures. *Microb Cell Fact*. 2017;16(1):220. doi:10.1186/s12934-017-0832-4
24. Marose S, Lindemann C, Scheper T. Two-dimensional fluorescence spectroscopy: A new tool for on-line bioprocess monitoring. *Biotechnol Prog*. 1998;14(1):63-74.
25. Faassen SM, Hitzmann B. Fluorescence spectroscopy and chemometric modeling for bioprocess monitoring. *Sensors*. 2015;15(5):10271-10291.

26. Zhang J, Greasham R. Chemically defined media for commercial fermentations. *App Microb Biotechnol*. 1999;51(4):407-421. doi:10.1007/s002530051411
27. McCloskey D, Utrilla J, Naviaux RK, Palsson BO, Feist AM. Fast Swinnex filtration (FSF): a fast and robust sampling and extraction method suitable for metabolomics analysis of cultures grown in complex media. *Metabolomics*. 2014;11(1):198-209. doi:10.1007/s11306-014-0686-2
28. Domröse A, Hage-Hülsmann J, Thies S, et al. *Pseudomonas putida* rDNA is a favored site for the expression of biosynthetic genes. *Sci Rep-UK*. 2019;9(1):1-13.
29. Hartmans S, Smits J, Van der Werf M, Volkering F, De Bont J. Metabolism of styrene oxide and 2-phenylethanol in the styrene-degrading *Xanthobacter strain* 124X. *App Environ Microb*. 1989;55(11):2850-2855.
30. Sambrook J, Fritsch E, Maniatis T. Molecular Cloning: A laboratory Manual. Cold Spring Harbor, New York: Cold Spring Harbor Laboratory Press. 1989;
31. Scheidle M, Dittrich B, Klinger J, Ikeda H, Klee D, Büchs J. Controlling pH in shake flasks using polymer-based controlled-release discs with pre-determined release kinetics. *BMC Biotechnol*. 2011;11(1):1-11.
32. Elbing K, Brent RJCPiMB. Media preparation and bacteriological tools. 2002;59(1):1.1. 1-1.1. 7.
33. Funke M, Diederichs S, Kensy F, Muller C, Büchs J. The baffled microtiter plate: increased oxygen transfer and improved online monitoring in small scale fermentations. *Biotech Bioeng*. 2009;103(6):1118-28. doi:10.1002/bit.22341
34. Anderlei T, Büchs J. Device for sterile online measurement of the oxygen transfer rate in shaking flasks. *Biochem Eng J*. 2001;7(2):157-162. doi:10.1016/S1369-703X(00)00116-9
35. Anderlei T, Zang W, Papaspyrou M, Büchs J. Online respiration activity measurement (OTR, CTR, RQ) in shake flasks. *Biochem Eng J*. 2004;17(3):187-194. doi:10.1016/S1369-703X(03)00181-5
36. Brass HCU, Klein AS, Nyholt S, Classen T, Pietruszka J. Condensing Enzymes from *Pseudoalteromonadaceae* for Prodiginine Synthesis. *Adv Synth Catal*. 2019;doi:10.1002/adsc.201900183
37. Samorski M, Müller-Newen G, Büchs J. Quasi-continuous combined scattered light and fluorescence measurements: a novel measurement technique for shaken microtiter plates. *Biotech Bioeng*. 2005;92(1):61-8. doi:10.1002/bit.20573
38. Loeschcke A, Markert A, Wilhelm S, et al. TREX: a universal tool for the transfer and expression of biosynthetic pathways in bacteria. *ACS Synth Biol*. 2013;2(1):22-33.
39. Belda E, Van Heck RG, José Lopez-Sanchez M, et al. The revisited genome of *Pseudomonas putida* KT2440 enlightens its value as a robust metabolic chassis. *Environ Microbiol*. 2016;18(10):3403-3424. doi:10.1111/1462-2920.13230
40. Nelson K, Weinel C, Paulsen I, et al. Complete genome sequence and comparative analysis of the metabolically versatile *Pseudomonas putida* KT2440. *Environ Microbiol*. 2002;4(12):799-808.
41. Bosdriesz E, Molenaar D, Teusink B, Bruggeman FJ. How fast-growing bacteria robustly tune their ribosome concentration to approximate growth-rate maximization. *FEBS J*. 2015;282(10):2029-2044. doi:10.1111/febs.13258
42. Duan J, Reimer L, Heikkila JJ, Glick BR. Differential expression of the seven rRNA operon promoters from the plant growth-promoting bacterium *Pseudomonas sp*. UW4. *FEMS Microbiol Lett*. 2014;361(2):181-189.
43. Kurylo CM, Parks MM, Juette MF, et al. Endogenous rRNA sequence variation can regulate stress response gene expression and phenotype. *Cell Rep*. 2018;25(1):236-248. e6.
44. Schleheck D, Barraud N, Klebensberger J, et al. *Pseudomonas aeruginosa* PAO1 preferentially grows as aggregates in liquid batch cultures and disperses upon starvation. *PLOS ONE*. 2009;4(5):e5513. doi:10.1371/journal.pone.0005513
45. Lamm R, Jäger VD, Heyman B, et al. Detailed small-scale characterization and scale-up of active YFP inclusion body production with *Escherichia coli* induced by a tetrameric coiled coil domain. *J Biosci Bioeng*. 2020;129(6):730-740. doi:https://doi.org/10.1016/j.jbiosc.2020.02.003
46. You Z, Liu X, Zhang S, Wang Y. Characterization of a prodigiosin synthetase PigC from *Serratia marcescens* jx-1 and its application in prodigiosin analogue synthesis. *Biochem Eng J*. 2018;134:1-11. doi:10.1016/j.bej.2018.01.034
47. Harris AK, Williamson NR, Slater H, et al. The *Serratia* gene cluster encoding biosynthesis of the red antibiotic, prodigiosin, shows species-and strain-dependent genome context variation. *Microbiology+*. 2004;150(11):3547-3560.
48. Brands S, Brass HUC, Klein AS, Pietruszka J, Ruff AJ, Schwaneberg U. A colourimetric high-throughput screening system for directed evolution of prodigiosin ligase PigC. *Chem Commun*. 2020;56(61):8631-8634. doi:10.1039/d0cc02181d
49. Brands S, Sikkens JG, Davari MD, et al. Understanding substrate binding and the role of gatekeeping residues in PigC access tunnels. *Chem Commun*. 2021;57(21):2681-2684. doi:10.1039/d0cc08226k
50. Cook TB, Jacobson TB, Venkataraman MV, et al. Stepwise genetic engineering of *Pseudomonas putida* enables robust heterologous production of prodigiosin and glidobactin A. *Metab Eng*. Sep 2021;67:112-124. doi:10.1016/j.ymben.2021.06.004

1. Fürstner A. Chemie und Biologie des Roseophilins und der Prodigiosin-Alkaloide: 2500 Jahre imÜberblick. *Angewandte Chemie*. 2003;115(31):3706-3728. doi:10.1002/ange.200300582
2. Hu DX, Withall DM, Challis GL, Thomson RJ. Structure, Chemical Synthesis, and Biosynthesis of Prodiginine Natural Products. *Chemical Reviews*. Jul 27 2016;116(14):7818-53. doi:10.1021/acs.chemrev.6b00024
3. Williamson NR, Fineran PC, Leeper FJ, Salmond GP. The biosynthesis and regulation of bacterial prodiginines. *Nature Reviews Microbiology* Dec 2006;4(12):887-99. doi:10.1038/nrmicro1531
4. Han R, Xiang R, Li J, Wang F, Wang C. High-level production of microbial prodigiosin: A review. *J Basic Microbiol*. Jun 2021;61(6):506-523. doi:10.1002/jobm.202100101
5. Habash SS, Brass HU, Klein AS, et al. Novel prodiginine derivatives demonstrate bioactivities on plants, nematodes, and fungi. *Frontiers in Plant Science*. 2020;11
6. Klein AS, Domröse A, Bongen P, et al. New prodigiosin derivatives obtained by mutasynthesis in Pseudomonas putida. *ACS synthetic biology*. 2017;6(9):1757-1765.
7. Klein AS, Brass HUC, Klebl DP, et al. Preparation of Cyclic Prodiginines by Mutasynthesis in *Pseudomonas putida* KT2440. *ChemBioChem*. Jul 16 2018;19(14):1545-1552. doi:10.1002/cbic.201800154
8. Zhao C, Qiu SZ, He J, et al. Prodigiosin impairs autophagosome-lysosome fusion that sensitizes colorectal cancer cells to 5-fluorouracil-induced cell death. *Cancer Lett*. Jul 1 2020;481:15-23. doi:10.1016/j.canlet.2020.03.010
9. Papireddy K, Smilkstein M, Kelly JX, et al. Antimalarial activity of natural and synthetic prodiginines. *Journal of Medicinal Chemistry*. 2011;54(15):5296-5306.
10. Stankovic N, Senerovic L, Ilic-Tomic T, Vasiljevic B, Nikodinovic-Runic J. Properties and applications of undecylprodigiosin and other bacterial prodigiosins. *Appl Microbiol Biotechnol*. 2014/05/01 2014;98(9):3841-3858. doi:10.1007/s00253-014-5590-1
11. Pérez-Tomás R, Montaner B, Llagostera E, Soto-Cerrato V. The prodigiosins, proapoptotic drugs with anticancer properties. *Biochemical Pharmacology*. 2003;66(8):1447-1452.
12. Berning L, Schlütermann D, Friedrich A, et al. Prodigiosin Sensitizes Sensitive and Resistant Urothelial Carcinoma Cells to Cisplatin Treatment. *Molecules*. 2021;26(5):1294. doi:10.3390/molecules26051294
13. Paul T, Bandyopadhyay TK, Mondal A, Tiwari ON, Muthuraj M, Bhunia B. A comprehensive review on recent trends in production, purification, and applications of prodigiosin. *Biomass Conversion and Biorefinery*. 2020;doi:10.1007/s13399-020-00928-2
14. Domröse A, Klein AS, Hage-Hülsmann J, et al. Efficient recombinant production of prodigiosin in *Pseudomonas putida*. *Front Microbiol*. 2015/09/15/ 2015;6doi:10.3389/fmicb.2015.00972
15. Dos Santos VA, Heim S, Moore ER, Stratz M, Timmis KN. Insights into the genomic basis of niche specificity of Pseudomonas putida KT2440. *Environ Microbiol*. Dec 2004;6(12):1264-86. doi:10.1111/j.1462-2920.2004.00734.x
16. Fernández M, Duque E, Pizarro-Tobías P, Van Dillewijn P, Wittich RM, Ramos JL. Microbial responses to xenobiotic compounds. Identification of genes that allow *Pseudomonas putida* KT2440 to cope with 2, 4, 6-trinitrotoluene. *Microbial Biotechnology*. 2009;2(2):287-294.
17. Tenconi E, Guichard P, Motte P, Matagne A, Rigali S. Use of red autofluorescence for monitoring prodiginine biosynthesis. *Journal of Microbiological Methods*. 2013/05// 2013;93(2):138-143. doi:10.1016/j.mimet.2013.02.012
18. Andreyeva IN, Ogorodnikova TI. Pigmentation of Serratia marcescens and spectral properties of prodigiosin. *Microbiology*. 2015/01// 2015;84(1):28-33. doi:10.1134/S0026261715010026
19. Aboras SI, Korany MA, Abdine HH, Ragab MAA, El Diwany A, Agwa MM. HPLC with fluorescence detection for the bioanalysis and pharmacokinetic study of Doxorubicin and Prodigiosin loaded on eco-friendly casein nanomicelles in rat plasma. *J Chromatogr B Analyt Technol Biomed Life Sci*. Dec 15 2021;1187:123043. doi:10.1016/j.jchromb.2021.123043
20. Geinitz B, Rehmann L, Büchs J, Regestein L. Noninvasive tool for optical online monitoring of individual biomass concentrations in a defined coculture. *Biotechnol Bioeng*. Apr 2020;117(4):999-1011. doi:10.1002/bit.27256
21. Wandrey G, Bier C, Binder D, et al. Light-induced gene expression with photocaged IPTG for induction profiling in a high-throughput screening system. *Microbial Cell Factories*. 2016/12// 2016;15(1)doi:10.1186/s12934-016-0461-3
22. Ladner T, Held M, Flitsch D, Beckers M, Büchs J. Quasi-continuous parallel online scattered light, fluorescence and dissolved oxygen tension measurement combined with monitoring of the oxygen transfer rate in each well of a shaken microtiter plate. *Microbial Cell Factories*. Dec 3 2016;15(1):206. doi:10.1186/s12934-016-0608-2
23. Mühlmann M, Forsten E, Noack S, Büchs J. Optimizing recombinant protein expression via automated induction profiling in microtiter plates at different temperatures. *Microbial Cell Factories*. Nov 28 2017;16(1):220. doi:10.1186/s12934-017-0832-4
24. Marose S, Lindemann C, Scheper T. Two-dimensional fluorescence spectroscopy: A new tool for on-line bioprocess monitoring. *Biotechnol Prog*. 1998;14(1):63-74.
25. Faassen SM, Hitzmann B. Fluorescence spectroscopy and chemometric modeling for bioprocess monitoring. *Sensors*. 2015;15(5):10271-10291.
26. Zhang J, Greasham R. Chemically defined media for commercial fermentations. *Appl Microbiol Biotechnol*. 1999/04/01 1999;51(4):407-421. doi:10.1007/s002530051411
27. McCloskey D, Utrilla J, Naviaux RK, Palsson BO, Feist AM. Fast Swinnex filtration (FSF): a fast and robust sampling and extraction method suitable for metabolomics analysis of cultures grown in complex media. *Metabolomics*. 2014;11(1):198-209. doi:10.1007/s11306-014-0686-2

28. Domröse A, Hage-Hülsmann J, Thies S, et al. Pseudomonas putida rDNA is a favored site for the expression of biosynthetic genes. *Scientific reports*. 2019;9(1):1-13.
29. Hartmans S, Smits J, Van der Werf M, Volkering F, De Bont J. Metabolism of styrene oxide and 2-phenylethanol in the styrene-degrading *Xanthobacter strain* 124X. *Appl Environ Microbiol*. 1989;55(11):2850-2855.
30. Sambrook J, Fritsch E, Maniatis T. Molecular Cloning: A laboratory Manual. Cold Spring Harbor, New York: Cold Spring Harbor Laboratory Press. 1989;
31. Scheidle M, Dittrich B, Klinger J, Ikeda H, Klee D, Büchs J. Controlling pH in shake flasks using polymer-based controlled-release discs with pre-determined release kinetics. *BMC Biotechnology*. 2011;11(1):1-11.
32. Elbing K, Brent RJCPiMB. Media preparation and bacteriological tools. 2002;59(1):1.1. 1-1.1. 7.
33. Funke M, Diederichs S, Kensy F, Muller C, Büchs J. The baffled microtiter plate: increased oxygen transfer and improved online monitoring in small scale fermentations. *Biotechnol Bioeng*. Aug 15 2009;103(6):1118-28. doi:10.1002/bit.22341
34. Anderlei T, Büchs J. Device for sterile online measurement of the oxygen transfer rate in shaking flasks. *Biochemical Engineering Journal*. 2001;7(2):157-162. doi:10.1016/S1369-703X(00)00116-9
35. Anderlei T, Zang W, Papaspyrou M, Büchs J. Online respiration activity measurement (OTR, CTR, RQ) in shake flasks. *Biochemical Engineering Journal*. 2004;17(3):187-194. doi:10.1016/S1369-703X(03)00181-5
36. Brass HUC, Klein AS, Nyholt S, Classen T, Pietruszka J. Condensing Enzymes from *Pseudoalteromonadaceae* for Prodiginine Synthesis. *Advanced Synthesis & Catalysis*. 2019;doi:10.1002/adsc.201900183
37. Samorski M, Müller-Newen G, Büchs J. Quasi-continuous combined scattered light and fluorescence measurements: a novel measurement technique for shaken microtiter plates. *Biotechnol Bioeng*. Oct 5 2005;92(1):61-8. doi:10.1002/bit.20573
38. Loeschcke A, Markert A, Wilhelm S, et al. TREX: a universal tool for the transfer and expression of biosynthetic pathways in bacteria. *ACS synthetic biology*. 2013;2(1):22-33.
39. Belda E, Van Heck RG, José Lopez-Sanchez M, et al. The revisited genome of *Pseudomonas putida* KT2440 enlightens its value as a robust metabolic chassis. *Environmental Microbiology*. 2016;18(10):3403-3424. doi:10.1111/1462-2920.13230
40. Nelson K, Weinel C, Paulsen I, et al. Complete genome sequence and comparative analysis of the metabolically versatile *Pseudomonas putida* KT2440. *Environmental Microbiology*. 2002;4(12):799-808.
41. Bosdriesz E, Molenaar D, Teusink B, Bruggeman FJ. How fast-growing bacteria robustly tune their ribosome concentration to approximate growth-rate maximization. *The FEBS Journal*. 2015;282(10):2029-2044. doi:10.1111/febs.13258
42. Duan J, Reimer L, Heikkila JJ, Glick BR. Differential expression of the seven rRNA operon promoters from the plant growth-promoting bacterium *Pseudomonas sp.* UW4. *FEMS microbiology letters*. 2014;361(2):181-189.
43. Kurylo CM, Parks MM, Juette MF, et al. Endogenous rRNA sequence variation can regulate stress response gene expression and phenotype. *Cell Reports*. 2018;25(1):236-248. e6.
44. Schleheck D, Barraud N, Klebensberger J, et al. *Pseudomonas aeruginosa* PAO1 preferentially grows as aggregates in liquid batch cultures and disperses upon starvation. *PLOS ONE*. 2009;4(5):e5513. doi:10.1371/journal.pone.0005513
45. Lamm R, Jäger VD, Heyman B, et al. Detailed small-scale characterization and scale-up of active YFP inclusion body production with Escherichia coli induced by a tetrameric coiled coil domain. *J Biosci Bioeng*. 2020/06/01/ 2020;129(6):730-740. doi:https://doi.org/10.1016/j.jbiosc.2020.02.003
46. You Z, Liu X, Zhang S, Wang Y. Characterization of a prodigiosin synthetase PigC from *Serratia marcescens* jx-1 and its application in prodigiosin analogue synthesis. *Biochemical Engineering Journal*. 2018;134:1-11. doi:10.1016/j.bej.2018.01.034
47. Harris AK, Williamson NR, Slater H, et al. The *Serratia* gene cluster encoding biosynthesis of the red antibiotic, prodigiosin, shows species-and strain-dependent genome context variation. *Microbiology*. 2004;150(11):3547-3560.
48. Brands S, Brass HUC, Klein AS, Pietruszka J, Ruff AJ, Schwaneberg U. A colourimetric high-throughput screening system for directed evolution of prodigiosin ligase PigC. *Chemical Communications*. Aug 7 2020;56(61):8631-8634. doi:10.1039/d0cc02181d
49. Brands S, Sikkens JG, Davari MD, et al. Understanding substrate binding and the role of gatekeeping residues in PigC access tunnels. *Chemical Communications*. Mar 11 2021;57(21):2681-2684. doi:10.1039/d0cc08226k
50. Cook TB, Jacobson TB, Venkataraman MV, et al. Stepwise genetic engineering of *Pseudomonas putida* enables robust heterologous production of prodigiosin and glidobactin A. *Metab Eng*. Sep 2021;67:112-124. doi:10.1016/j.ymben.2021.06.004

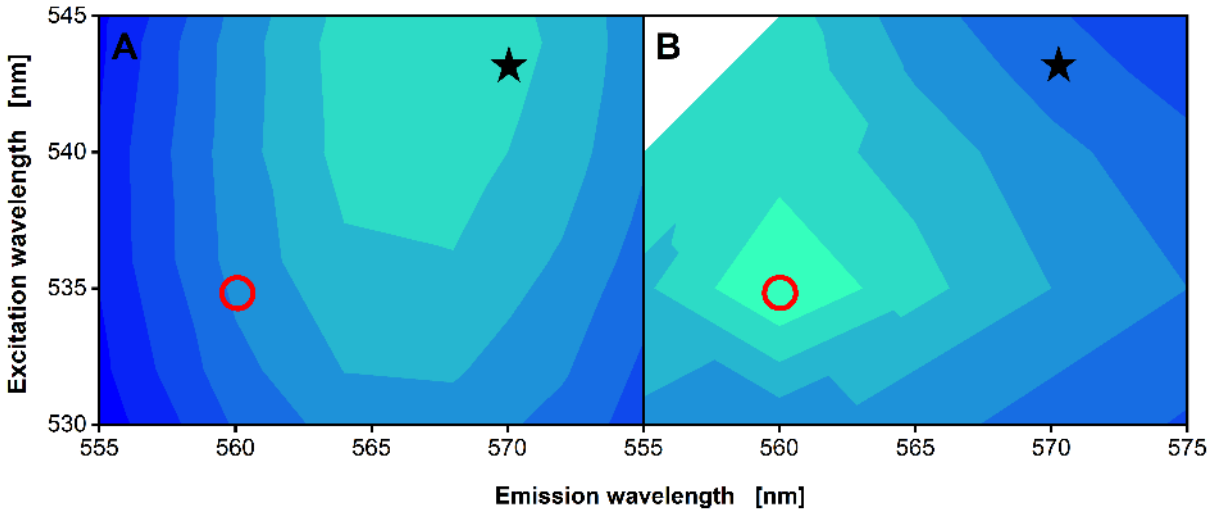

Figure 1: 2D fluorescent spectrum of 1 mg/L prodigiosin (A) in DMSO (pH 7) in a quartz cuvette and (B) in culture medium after 12 hours of cultivation in a 48-well Flowerplate. Cultivation of *P. putida* pig-r2 in modified M63 mineral medium (16 g/L glucose, pH 7) was performed in triplicate. Stars mark the wavelength combination (ex/em) where the strongest fluorescence of prodigiosin in DMSO was measured (ex/em: 543/570 nm). Circles mark the wavelength combination where strongest fluorescence of prodigiosin in culture medium was measured (ex/em: 535/560 nm).

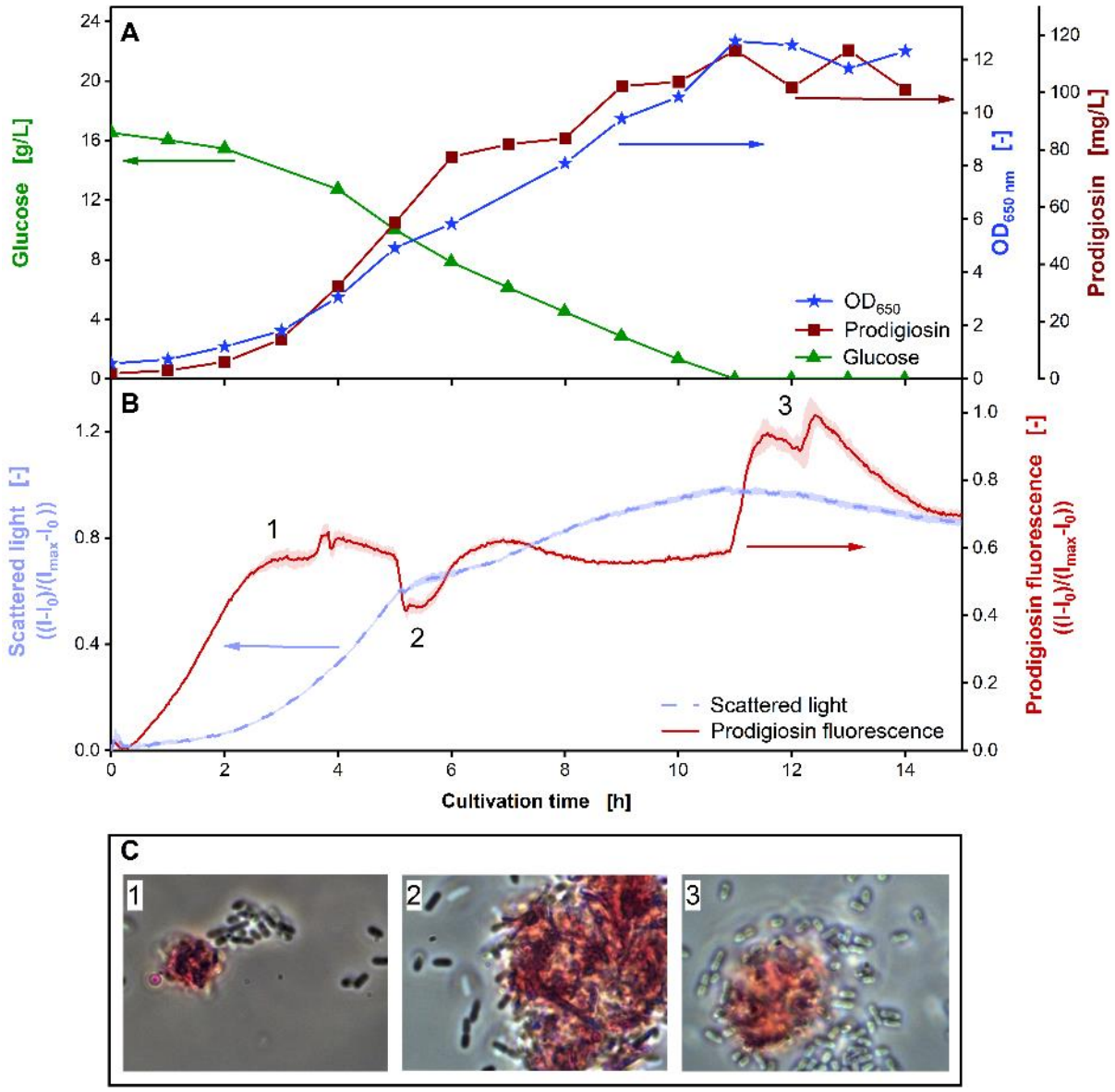

Figure 2: Growth characterization of *P. putida* pig-r2 using an in-house built device for fluorescence measurement in MTPs with additional determination of culture parameters. The offline parameters (A) are shown as the mean of biological duplicates (duplicates shown in Suppl. Fig. 5). Fluorescence and scattered light signals (B) were determined in biological triplicates; (C) shows microscopic images (1000 x magnification) at the time points marked with corresponding numbers in (B). At each sampling point, two wells of the MTP were used for analysis. Cultivation conditions of *P. putida* pig-r2: modified M63 mineral medium (16 g/L glucose, pH 7, 30 °C) (for details see 2.3). (B) shows the scattered light intensity (at ex/em 650/650 nm) and the prodigiosin fluorescence (at ex/em: 535/560 nm). The shadows of the

curves in (B) represent the standard deviation at each time point. Prodigiosin fluorescence and scattered light was normalized using Equation 1 to a reference cultivation performed with *P. putida* pig-r2 (for details see 2.4)

670

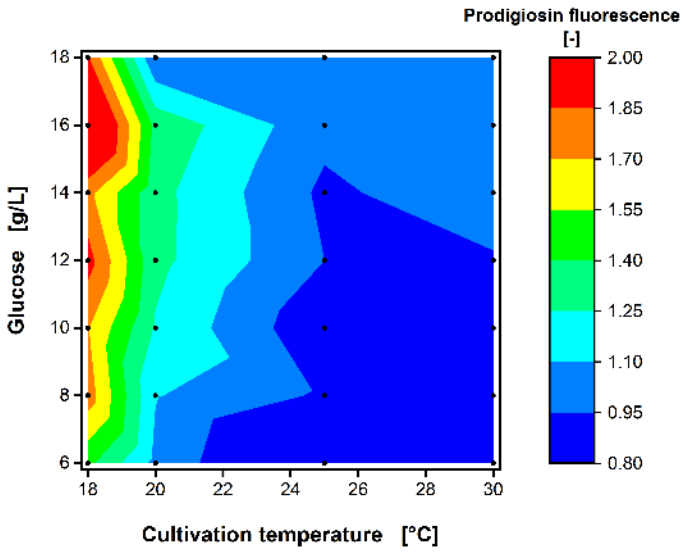

Figure 3: Normalized online measured prodigiosin fluorescence intensities of *P. putida* pig-r2 at different temperatures and glucose concentrations. Each black dot represents the mean of three cultivations. The normalized prodigiosin fluorescence intensities (at ex/em: 535/560 nm) shown were obtained at time point 3 during the cultivation, as defined in Figure 2 B. Cultivation conditions of *P. putida* pig-r2: modified M63 mineral medium (pH 7), (for details see 2.3). Prodigiosin fluorescence and scattered light was normalized with Equation 1 to a reference cultivation performed with *P. putida* pig-r2 (for details see 2.4)

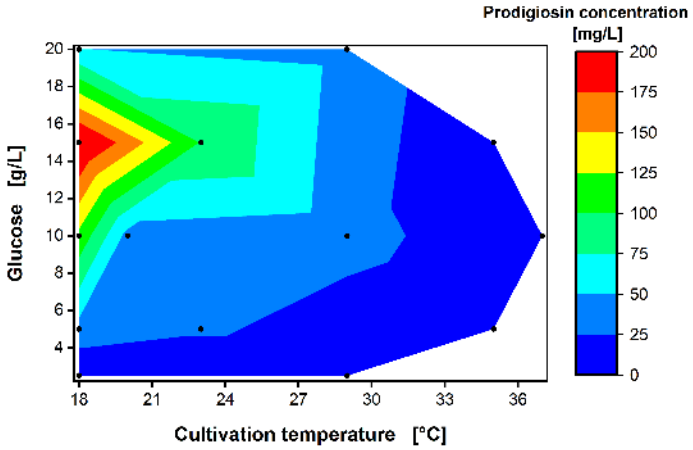

680

Figure 4: Offline measured absolute prodigiosin concentrations at different temperatures and glucose concentrations. Cultivation conditions of *P. putida* pig-r2: modified M63 mineral medium (pH 7), (for details see 2.3). The prodigiosin concentration was determined by measuring the absorption at 535 nm. Measurement was performed when all cultures reached
685 the stationary phase. Each of the black dots in the Figure resembles one cultivation.

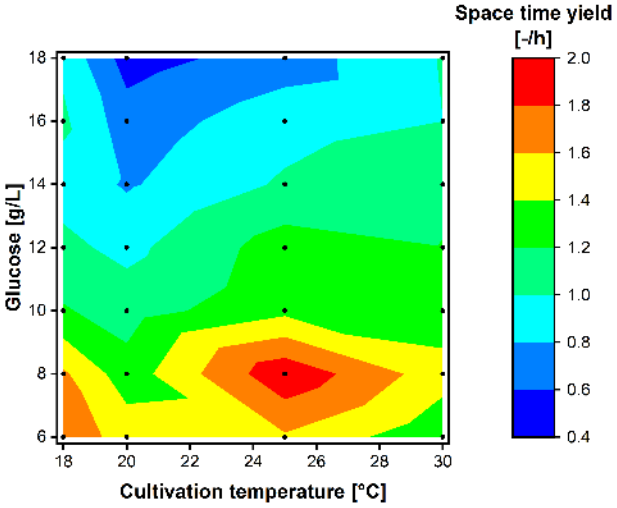

Figure 5: Space-time-yield (STY) at different temperatures and glucose concentrations. Each black dot represents the STY calculated from the mean of three cultivations. The STY was calculated from the normalized online measured prodigiosin fluorescence intensities (at ex/em: 535/560 nm), obtained at time point 3 during the cultivation, as defined in Figure 2 B. Cultivation conditions of *P. putida* pig-r2: modified M63 mineral medium (pH 7), (for details see 2.3). Prodigiosin fluorescence was normalized with Equation 1 to a reference cultivation performed with *P. putida* pig-r2 (for details see 2.4).